

$\rho(\omega) \rightarrow \pi^0\pi^0\gamma, \rho(\omega) \rightarrow \eta\pi^0\gamma$ decays in the local quark Nambu–Jona-Lasinio model

A. E. Radzhabov,* M. K. Volkov,† and N. G. Kornakov‡

Bogoliubov Laboratory of Theoretical Physics, Joint Institute for Nuclear Research, 141980 Dubna, Russia

(Dated: November 6, 2018)

The branching ratios and photon spectra of the rare processes $\rho(\omega) \rightarrow \pi^0\pi^0\gamma, \rho(\omega) \rightarrow \eta\pi^0\gamma$ are calculated in the framework of the standard local quark Nambu–Jona-Lasinio (NJL) model. Three types of diagrams are considered: the quark box and the pole diagrams with scalar ($\sigma, a_0(980)$) and vector (ρ, ω) mesons. The obtained estimations for the widths of the processes $\rho(\omega) \rightarrow \pi^0\pi^0\gamma$ are in satisfactory agreement with existing experimental data. Predictions are made for the widths of the processes $\rho(\omega) \rightarrow \eta\pi^0\gamma$.

I. INTRODUCTION

At the present time, there are many theoretical and experimental works devoted to investigation of the rare decay processes $\rho(\omega) \rightarrow \pi^0(\eta)\pi^0\gamma$. These processes are very interesting for studying the mechanism of chiral symmetry breaking of strong interaction of hadrons.

Recently, the branching ratios for the rare decays of ρ and ω mesons to the pair of pions have been measured with good accuracy by SND [1] and CMD-2 [2] collaborations at VEPP-2M e^+e^- collider (see table I where theoretical estimations and experimental results are given). The situation for decays with η meson in the final state is worse than for radiative two pion production, there is an estimation for the upper limit for the decay of ω -meson $\mathcal{B}(\omega \rightarrow \eta\pi^0\gamma) < 3.3 \times 10^{-5}$ at 90% C.L. only [2]. Therefore, the theoretical predictions for the decays of vector mesons into $\eta\pi^0\gamma$ are of large interest.

Indeed, there are many theoretical works devoted to the description of these processes in different models. For instance, in one of the first works devoted to the calculations of these decays, the vector meson dominance (VMD) model was used [3, 4]. Only diagrams with intermediate vector mesons were taken into account and only rough estimations of these processes were obtained. In 1992, in the framework of a similar model these processes were estimated more accurately and it was found that the VMD leads to too low values of the branching ratios [5] (see table 1). Lately in [6, 7, 8, 9] it was found that inclusion of diagrams with scalar meson exchange increases branching ratios, which leads to better agreement with experiment. There are different methods to take into account the effect of scalar meson exchange. One of them is connected with phenomenological inclusion of the scalar pole diagram with the mass and the width fixed from experiment [7, 8, 10]. This method of inclusion of the scalar meson leads to the breaking of chiral symmetry. Other methods taking into account scalar effects are connected with dynamical generation of the scalar meson after unitarization of pseudoscalar meson

TABLE I: Branching ratios for the processes $\rho \rightarrow \pi^0\pi^0\gamma$ and $\omega \rightarrow \pi^0\pi^0\gamma$ obtained in experiment (upper part) and theoretically(lower part).

	$\rho \rightarrow \pi^0\pi^0\gamma, 10^{-5}$	$\omega \rightarrow \pi^0\pi^0\gamma, 10^{-5}$
SND [1]	$4.1^{+1.0}_{-0.9} \pm 0.3$	$6.6^{+1.4}_{-1.3} \pm 0.6$
CMD-2 [2]	$5.2^{+1.5}_{-1.3} \pm 0.6$	$6.4^{+2.4}_{-2.0} \pm 0.8$
PDG [12]	4.4 ± 0.8	6.7 ± 1.1
[5]	1.1	2.8
[6]	4.2	4.7
[9]	3.8	4.5 ± 1.1
[11]	4.2	$3.5 - 4.6$
This work	4	8.3

TABLE II: Branching ratios for the processes $\rho \rightarrow \eta\pi^0\gamma$ and $\omega \rightarrow \eta\pi^0\gamma$ obtained theoretically.

	$\rho \rightarrow \eta\pi^0\gamma$	$\omega \rightarrow \eta\pi^0\gamma$
[5]	4×10^{-10}	1.6×10^{-7}
[6]	7.5×10^{-10}	3.3×10^{-7}
[10]	2.3×10^{-8}	5.72×10^{-7}
[11]	5.2×10^{-10}	9.7×10^{-8}
This work	1.64×10^{-9}	3.65×10^{-7}

loop diagrams [6] or based on linear sigma model [9, 11]. Let us note that in most these models it was necessary to use additional parameters for description of the above-mentioned rare decays of vector mesons.

In the present paper, we suggest using the well-known $U(3) \times U(3)$ local quark NJL model [13, 14, 15, 16, 17, 18, 19, 20, 21, 22, 23, 24, 25, 26, 27] for the description of decays of ρ, ω -mesons into a pair of neutral pseudoscalar mesons. The advantage of the model is that for descriptions of these processes it is not necessary to introduce any additional parameter. Three types of diagrams are taken into account: quark box and pole diagrams with intermediate scalar ($\sigma, a_0(980)$) and vector (ρ, ω) mesons. In addition, the estimations are given for the processes whose vertices appear in the amplitudes of pole diagrams.

The obtained results for the decay processes $\rho(\omega) \rightarrow \pi^0\pi^0\gamma$ are in satisfactory agreement with experimental data. Predictions for decay processes $\rho(\omega) \rightarrow \eta\pi^0\gamma$ do not contradict existing experiments.

*Electronic address: aradzh@theor.jinr.ru

†Electronic address: volkov@theor.jinr.ru

‡Electronic address: kornakov@theor.jinr.ru

TABLE III: Meson masses obtained in the model in comparison with experimental data [12].

	model	experiment
M_π	135	134.9766 ± 0.0006
M_K	495	497.648 ± 0.022
M_η	511	547.51 ± 0.18
$M_{\eta'}$	972	957.78 ± 0.14
M_ρ	775.5	775.5 ± 0.4
M_σ	516	400 – 1200
$M_{a_0}(980)$	785	984.7 ± 1.2
$M_{f_0}(980)$	1100	980 ± 10

II. MODEL PARAMETERS AND DESCRIPTION OF INTERMEDIATE PROCESSES

The $U(3) \times U(3)$ NJL model is based on the effective four-quark interaction in the scalar–pseudoscalar and vector–axial-vector channels and six-quark t'Hooft interaction. The weak interactions are introduced in the model with the help of redefining a kinetic quark term and electromagnetic interactions are introduced with help of VMD. Since the details of the model are described in many papers (see e.g. [18, 22, 24, 25, 26]), we give here only general characteristics of this model and parameters of the model which are needed for our calculations. The model contains the mechanism of spontaneous breaking of chiral symmetry and has six arbitrary parameters: constituent masses of nonstrange $m_u = m_d = 263$ MeV and strange $m_s = 407$ MeV quarks, $O(4)$ cut-off $\Lambda = 1.27$ GeV, the four-quark coupling constants in scalar–pseudoscalar $G_1 = 4.16$ GeV⁻² and vector–axial-vector $G_2 = 14.66$ GeV⁻² channels, and the six-quark t'Hooft coupling constant $K = 12.5$ GeV⁻⁵. The model parameters are defined as in [25, 26]¹ using experimental values of masses of the pion, kaon and ρ -meson, $\eta - \eta'$ mass difference, the weak pion decay constant $f_\pi = 92.4$ MeV, and the strong decay width $\rho \rightarrow \pi\pi$ ($g_\rho = 5.94$). As a result, in the NJL model it is possible to describe the mass spectrum and main strong and electroweak decays of pseudoscalar, scalar, vector, and axial-vector meson nonets [18, 19, 20, 21, 22, 23, 24, 25, 26, 28].

In the following we need a meson-quark coupling constant. The scalar meson coupling constant takes the form [18, 26, 27]

$$g_{a_0} = g_{\sigma_u} = [4I_2^\Lambda(m_u)]^{-1} = \frac{g_\rho}{\sqrt{6}}, \quad (1)$$

where $I_2^\Lambda(m)$ is logarithmically divergent integral

$$I_2^\Lambda(m) = \frac{N_c}{(2\pi)^4} \int d^4k \frac{\theta(\Lambda^2 - k^2)}{(k^2 + m^2)^2}. \quad (2)$$

After taking into account the $\pi - a_1$ transition there is additional renormalization of pion fields

$$g_\pi = g_{\eta_u} = g_{a_0} Z^{1/2}, \quad Z = \left(1 - \frac{6m_u^2}{M_{a_1}^2}\right)^{-1}. \quad (3)$$

From the weak pion decay $\pi \rightarrow \mu\nu$ the Goldberger-Treiman relation follows $f_\pi = m/g_\pi$. Physical isoscalar mesons are the mixed states of the pure nonstrange and strange states and t'Hooft interaction allows us to correctly describe this mixing. We define these states as

$$\begin{aligned} \eta &= -\eta_u \sin \bar{\theta} + \eta_s \cos \bar{\theta}, \\ \eta' &= \eta_u \cos \bar{\theta} + \eta_s \sin \bar{\theta}, \quad \bar{\theta} = \theta - \theta_0 \\ \sigma &= \sigma_u \cos \bar{\phi} - \sigma_s \sin \bar{\phi}, \\ f_0 &= \sigma_u \sin \bar{\phi} + \sigma_s \cos \bar{\phi}, \quad \bar{\phi} = \theta_0 - \phi \end{aligned} \quad (4)$$

where $\theta_0 \approx 35.3^\circ$ is the ideal mixing angle ($\text{ctg } \theta_0 = \sqrt{2}$), $\theta = -18.1$ and $\phi = 23.4$ are the singlet-octet mixing angles for pseudoscalar and scalar mesons [25]. Meson masses obtained in the model are given in table III.

The processes of rare decays of vector mesons are described by three types of diagrams (see fig. 1): quark box and diagrams with intermediate scalar and vector mesons.

Let us consider vertices that are contained in the resonance diagrams and calculate the corresponding physical processes.

The amplitude of the processes of strong decay of scalar mesons $a_0(980) \rightarrow \eta\pi$ and $\sigma \rightarrow \pi\pi$ expressed through the divergent integral $I_2^\Lambda(m)$ and has the form

$$\begin{aligned} g_{\sigma\pi\pi} &= 8 \cos \bar{\phi} g_{\sigma_u} g_\pi^2 I_2^\Lambda(m_u) = \cos \bar{\phi} \frac{2m_u^2 Z^{1/2}}{f_\pi}, \quad (5) \\ g_{a_0\eta\pi} &= -8 \sin \bar{\theta} g_{a_0} g_{\eta_u} g_\pi I_2^\Lambda(m_u) = -\sin \bar{\theta} \frac{2m_u^2 Z^{1/2}}{f_\pi}. \end{aligned}$$

The corresponding strong decay widths of scalar mesons takes the form

$$\begin{aligned} \Gamma_\sigma(s) &= \frac{3g_{\sigma\pi\pi}^2}{8\pi s} \sqrt{1 - \frac{4M_\pi^2}{s}}, \quad \Gamma_{a_0}(s) = \frac{g_{a_0\eta\pi}^2}{4\pi s} \times \quad (6) \\ &\times \sqrt{\left(1 - \frac{(M_\eta + M_\pi)^2}{s}\right) \left(1 - \frac{(M_\eta - M_\pi)^2}{s}\right)} \end{aligned}$$

As a result, the decay widths $a_0(980) \rightarrow \eta\pi$ and $\sigma \rightarrow \pi\pi$ are in agreement with experiment (see table IV).

The momentum dependent width of ρ -meson is

$$\Gamma_\rho(s) = \frac{g_\rho^2 s}{48\pi} \left(1 - \frac{4M_\pi^2}{s}\right)^{3/2}$$

¹ Note that in the present paper for definition of model parameters we have used recent experimental data [12] for ρ -meson mass and decays $\pi \rightarrow \mu\nu$, $\rho \rightarrow \pi\pi$.

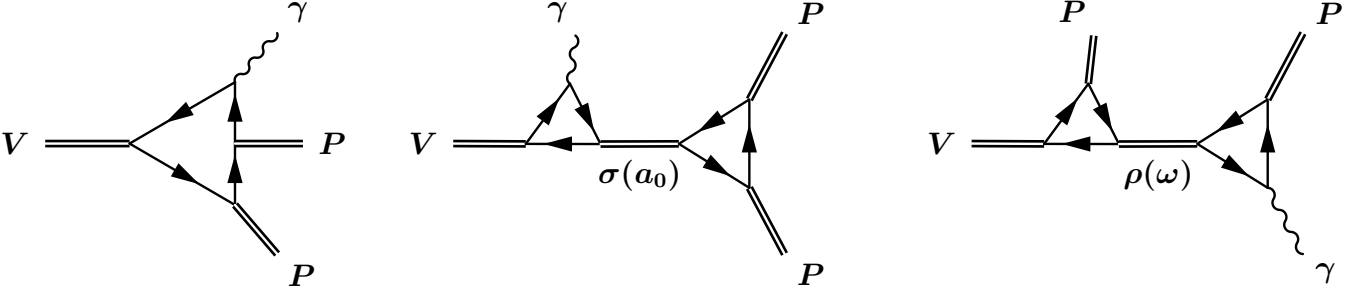


FIG. 1: Diagrams contributing to the amplitudes of the decays of vector mesons into pair pseudoscalar mesons and photon.

TABLE IV: Meson decays obtained in the model in comparison with experimental data [12].

	theory	experiment
$\rho \rightarrow \pi\pi$, MeV	149	149.4 ± 1.0
$\sigma \rightarrow \pi\pi$, MeV	582	600 – 1000
$a_0 \rightarrow \eta\pi$, MeV	105	50 – 100
$\omega \rightarrow 3\pi$, MeV	9.05	7.56 ± 0.07
$\rho^0 \rightarrow \pi^0\gamma$, KeV	86	90 ± 13
$\rho^0 \rightarrow \eta\gamma$, KeV	69	44 ± 5
$\omega \rightarrow \pi\gamma$, KeV	771	755^{+30}_{-26}
$\omega \rightarrow \eta\gamma$, KeV	7.68	4.16 ± 0.46

The decays $\rho(\omega) \rightarrow \pi\gamma$, $\rho(\omega) \rightarrow \eta\gamma$ are described by anomalous triangle diagrams. The amplitudes for the processes $\rho(\omega) \rightarrow \eta(\pi)\gamma$ have the form

$$A(VP\gamma) = C_{VPV} \frac{g_\rho}{8\pi f_\pi^2} \epsilon_{\mu\nu\alpha\beta} \epsilon_1^\mu \epsilon_2^\nu q_1^\alpha q_2^\beta, \quad (7)$$

where q_1, q_2 and $\epsilon_1^\mu, \epsilon_2^\nu$ are the momentum and the polarization vector of vector meson and photon, respectively. The factors C_{VPV} are: $C_{\rho\pi\gamma} = e$, $C_{\rho\eta\gamma} = -3\sin\bar{\theta}e$, $C_{\omega\pi\gamma} = 3e$, $C_{\omega\eta\gamma} = -\sin\bar{\theta}e$, $C_{\rho\pi\omega} = g_\rho$, $C_{\rho\eta\rho} = -\sin\bar{\theta}g_\rho$, $C_{\omega\eta\omega} = -\sin\bar{\theta}g_\rho$. Note that decays of $\rho(\omega) \rightarrow \pi\gamma$ are in good agreement with experiment, whereas $\rho(\omega) \rightarrow \eta\gamma$ are in qualitative agreement with experiment.

At the end of this section, we should like to note that the main decay of ω -meson $\omega \rightarrow 3\pi$ is slightly above experimental data. In [29] this process is calculated using form-factor in the $\rho\pi\pi$ vertex, which leads to better agreement with experiment. Compilation of model predictions for widths of different decay processes is given in table IV together with experimental results.

III. DECAYS $\rho(\omega) \rightarrow \pi^0(\eta)\pi^0\gamma$

The amplitudes for the $\rho(\omega) \rightarrow \pi^0(\eta)\pi^0\gamma$ decay processes are described by three types of diagrams, see fig. 1. Possible combinations of intermediate states for the diagrams with meson exchanges are the following:

- $\rho \rightarrow (\sigma\gamma \text{ and } \omega\pi^0) \rightarrow \pi^0\pi^0\gamma$

- $\omega \rightarrow (\sigma\gamma \text{ and } \rho\pi^0) \rightarrow \pi^0\pi^0\gamma$
- $\rho \rightarrow (a_0\gamma \text{ and } \omega\pi^0 \text{ and } \rho\eta) \rightarrow \eta\pi^0\gamma$
- $\omega \rightarrow (a_0\gamma \text{ and } \rho\pi^0 \text{ and } \omega\eta) \rightarrow \eta\pi^0\gamma$

Let us consider these contributions in detail.

The quark box diagram has the form [30]

$$A_{\text{box}}^{\mu\nu} = C_{VPP\gamma} \frac{5eg_\rho}{(6\pi f_\pi)^2} (g^{\mu\nu}(p \cdot q_1) - p^\nu q_3^\mu),$$

where p, q_3 are the momentum of vector meson and photon; factors $C_{VPP\gamma}$ are $C_{\rho\pi^0\pi^0\gamma} = 1$, $C_{\omega\pi^0\pi^0\gamma} = 1/3$, $C_{\rho\eta\pi^0\gamma} = -\sin\bar{\theta}/3$, $C_{\omega\eta\pi^0\gamma} = -\sin\bar{\theta}$.

Scalar exchange diagrams have the same tensor structure as the quark box. Therefore it is convenient to combine these amplitudes

$$A_{\text{box+scalar}}^{\mu\nu} = C_{VPP\gamma} \frac{5eg_\rho}{(6\pi f_\pi)^2} (g^{\mu\nu}(p \cdot q) - p^\nu q^\mu) \times \left(1 - \frac{4m_u^2 C_S}{m_S^2 - s - im_S \Gamma_S(s)} \right), \quad (8)$$

where \mathcal{S} means scalar σ or $a_0(980)$ meson; the factor C_S is $C_{a_0} = 1$ and $C_\sigma = \cos\bar{\phi}$; $s = (p - q_3)^2 = (q_1 + q_2)^2$, where q_1 and q_2 are the momentum of pseudoscalar mesons.

The amplitudes with the vector meson (ρ, ω) exchanges consists of two quark triangles of anomalous type and the vector meson propagator. It gives the following contributions:

$$A_{\text{vector}}^{\mu\nu} = \frac{g_\rho}{(8\pi f_\pi^2)^2} \epsilon_{\mu\delta\alpha\beta} \epsilon_{\nu\tau\lambda} g^{\delta\gamma} p^\alpha q_3^\lambda \times \left[\frac{C_{VP_1V'} C_{V'P_2\gamma} l_1^\beta l_1^\tau}{m_{V'}^2 - l_1^2 - im_{V'} \Gamma_{V'}(l_1^2)} + \frac{C_{VP_1V''} C_{V''P_2\gamma} l_2^\beta l_2^\tau}{m_{V''}^2 - l_2^2 - im_{V''} \Gamma_{V''}(l_2^2)} \right], \quad (9)$$

where V', V'' are intermediate mesons and $l_1 = p - q_1$, $l_2 = p - q_2$. The possible combinations of factors for different decays are

- $\rho \rightarrow \pi^0\pi^0\gamma$

$$C_{VP_1V'} = C_{VP_1V''} = C_{\rho\pi\omega}, \quad C_{V'P_2\gamma} = C_{V''P_2\gamma} = C_{\omega\pi\gamma}$$

- $\omega \rightarrow \pi^0\pi^0\gamma$

$$C_{VP_1V'} = C_{VP_1V''} = C_{\rho\pi\omega}, \quad C_{V'P_2\gamma} = C_{V''P_2\gamma} = C_{\rho\pi\gamma}$$

TABLE V: Different contributions to the branching ratios for the processes of rare decay of vector mesons.

process	box+scalar	vector	interference	total
$\rho \rightarrow \pi^0 \pi^0 \gamma, 10^{-5}$	2.36	1.37	0.27	4.0
$\omega \rightarrow \pi^0 \pi^0 \gamma, 10^{-5}$	4.97	2.86	0.47	8.3
$\rho \rightarrow \eta \pi^0 \gamma, 10^{-9}$	0.56	0.85	0.23	1.64
$\omega \rightarrow \eta \pi^0 \gamma, 10^{-7}$	1.22	1.92	0.51	3.65

- $\rho \rightarrow \eta \pi^0 \gamma$

$$C_{VP_1 V'} = C_{\rho \pi \omega}, C_{VP_1 V''} = C_{\rho \eta \rho},$$

$$C_{V' P_2 \gamma} = C_{\omega \eta \gamma}, C_{V'' P_2 \gamma} = C_{\omega \pi \gamma}$$

- $\omega \rightarrow \eta \pi^0 \gamma$

$$C_{VP_1 V'} = C_{\rho \pi \omega}, C_{VP_1 V''} = C_{\omega \eta \omega},$$

$$C_{V' P_2 \gamma} = C_{\rho \pi \gamma}, C_{V'' P_2 \gamma} = C_{\omega \pi \gamma}$$

The width of ρ meson is given by eq. (7) and the width of ω meson is ignored.

The decay widths have the form

$$\Gamma_{V \pi^0 P \gamma} = \frac{1}{192 \pi^3 M_V} \int_0^{E_\gamma^{\max}} dE_\gamma \int_{E_\pi^{\min}}^{E_\pi^{\max}} dE_\pi |A_{V \pi^0 P \gamma}|^2,$$

$$E_\gamma^{\max} = \frac{M_V^2 - (M_\pi + M_P)^2}{2M_V}, \quad (10)$$

$$E_\pi^{\min, \max} = \frac{1}{2M_V(2E_\gamma - M_V)} \times$$

$$\times \left[(M_V - E_\gamma)(M_V(2E_\gamma - M_V) + (M_\pi^2 - M_P^2)) \pm E_\gamma \times \right.$$

$$\times (M_V(2E_\gamma - M_V) + (M_\pi - M_P)^2)^{1/2} \times$$

$$\left. \times (M_V(2E_\gamma - M_V) + (M_\pi + M_P)^2)^{1/2} \right]$$

where E_γ, E_π are energies of photon and pion, P means pion or η -meson (in case of pion additional factor 1/2 required).

The resulting branching ratios for rare processes are given in table V.

The photon spectra for widths the of the decays $\rho \rightarrow \pi^0 \pi^0 \gamma, \omega \rightarrow \pi^0 \pi^0 \gamma, \rho \rightarrow \eta \pi^0 \gamma, \omega \rightarrow \eta \pi^0 \gamma$ are shown in figs. 2, 3, 4, 5, respectively .

IV. DISCUSSION AND CONCLUSION

The performed calculations show that the decays widths of the processes $\rho(\omega) \rightarrow \pi^0 \pi^0 \gamma$ are in satisfactory agreement with existing experimental data. The branching ratio for the process $\omega \rightarrow \eta \pi^0 \gamma$ also does not contradict the existing experimental limit. Comparing our result with predictions of different theoretical models we can see that decays width with η -meson is significantly different. Therefore, obtaining the experimental data for these processes is a very topical problem. We would like to emphasize that in our calculation of rare processes in the framework of the standard NJL model no additional parameters are used.

Note, that in difference with poor experimental data on decays $\rho(\omega) \rightarrow \eta \pi^0 \gamma$ the situation is much better for decays of ϕ -meson where rich and accurate experimental information exists. In future we plan to investigate different decays of ϕ -meson. We hope to obtain reasonable results because predictions of the NJL model [18, 22, 24] for the ϕ -meson mass and the main strong decay into two kaons are in satisfactory agreement with experiment [12].

Acknowledgments

The authors thank A. E. Dorokhov and V. L. Yudichev for useful discussions. The authors acknowledge the support of the Russian Foundation for Basic Research, under contract 05-02-16699.

-
- [1] M. N. Achasov et al., Phys. Lett. **B537**, 201 (2002), hep-ex/0205068.
- [2] R. R. Akhmetshin et al. (CMD2), Phys. Lett. **B580**, 119 (2004), hep-ex/0310012.
- [3] P. Singer, Phys. Rev. **128**, 2789 (1962).
- [4] P. Singer, Phys. Rev. **130**, 2441 (1963).
- [5] A. Bramon, A. Grau, and G. Pancheri, Phys. Lett. **B283**, 416 (1992).
- [6] J. E. Palomar, S. Hirenzaki, and E. Oset, Nucl. Phys. **A707**, 161 (2002), hep-ph/0111308.
- [7] A. Gokalp and O. Yilmaz, Phys. Lett. **B494**, 69 (2000), nucl-th/0008011.
- [8] A. Gokalp and O. Yilmaz, Phys. Lett. **B508**, 25 (2001), nucl-th/0006044.
- [9] A. Bramon, R. Escribano, J. L. Lucio Martinez, and M. Napsuciale, Phys. Lett. **B517**, 345 (2001), hep-ph/0105179.
- [10] A. Kucukarslan and S. Solmaz, Phys. Rev. **D70**, 053004 (2004), hep-ph/0405151.
- [11] R. Escribano, Phys. Rev. **D74**, 114020 (2006), hep-ph/0606314.
- [12] W.-M. Yao et al., Journal of Physics G **33**, 1+ (2006), URL <http://pdg.lbl.gov>.
- [13] Y. Nambu and G. Jona-Lasinio, Phys. Rev. **122**, 345 (1961).
- [14] T. Eguchi, Phys. Rev. **D14**, 2755 (1976).
- [15] M. K. Volkov and D. Ebert, Yad. Fiz. **36**, 1265 (1982).
- [16] D. Ebert and M. K. Volkov, Z. Phys. **C16**, 205 (1983).
- [17] M. K. Volkov, Annals Phys. **157**, 282 (1984).
- [18] M. K. Volkov, Sov.J.Part. and Nuclei **17**, 186 (1986).

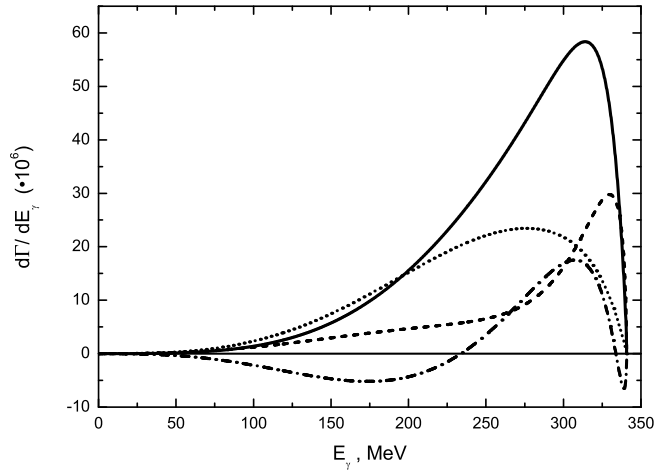


FIG. 2: Photon spectra for width of the decay $\rho \rightarrow \pi^0 \pi^0 \gamma$. The different contribution are shown: box+scalar meson contributions(dots), vector meson contributions(short dash), interference(dash-dot) and total spectra(continuous line).

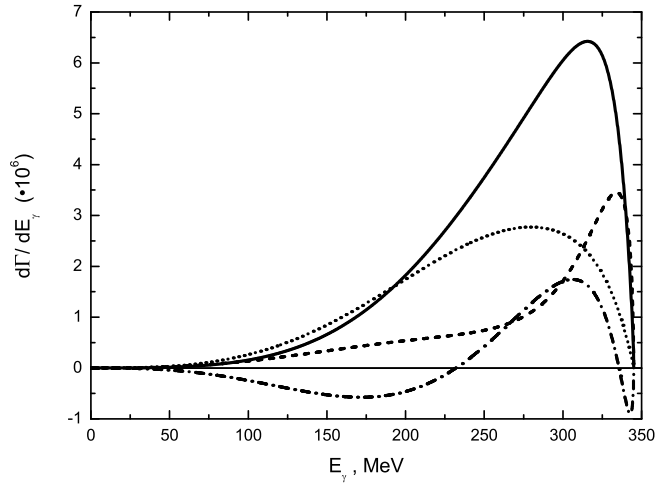


FIG. 3: Photon spectra for width of the decay $\omega \rightarrow \pi^0 \pi^0 \gamma$. The different contribution are shown: box+scalar meson contributions(dots), vector meson contributions(short dash), interference(dash-dot) and total spectra(continuous line).

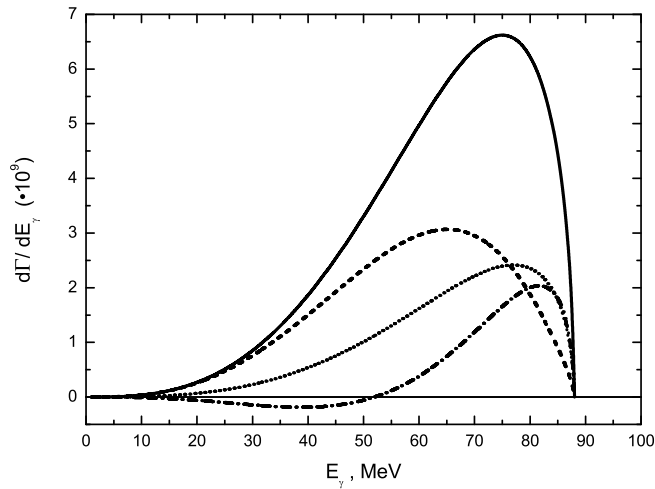


FIG. 4: Photon spectra for width of the decay $\rho \rightarrow \eta \pi^0 \gamma$. The different contribution are shown: box+scalar meson contributions(dots), vector meson contributions(short dash), interference(dash-dot) and total spectra(continuous line).

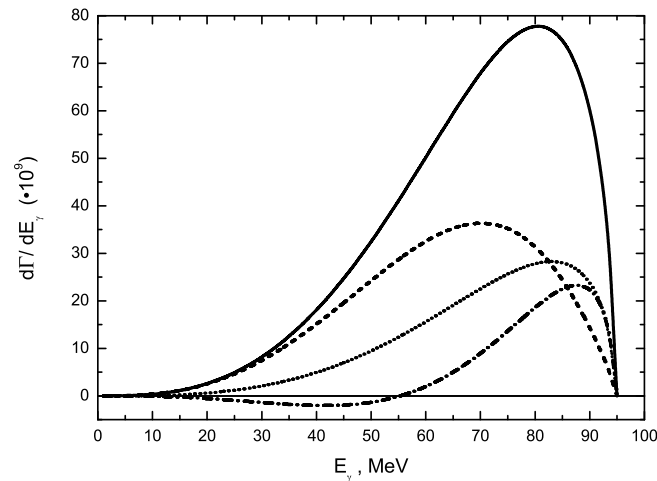


FIG. 5: Photon spectra for width of the decay $\omega \rightarrow \eta\pi^0\gamma$. The different contribution are shown: box+scalar meson contributions(dots), vector meson contributions(short dash), interference(dash-dot) and total spectra(continuous line).

- [19] D. Ebert and H. Reinhardt, Nucl. Phys. **B271**, 188 (1986).
- [20] S. Klimt, M. Lutz, U. Vogl, and W. Weise, Nucl. Phys. **A516**, 429 (1990).
- [21] S. P. Klevansky, Rev. Mod. Phys. **64**, 649 (1992).
- [22] M. K. Volkov, Phys. Part. Nucl. **24**, 35 (1993).
- [23] T. Hatsuda and T. Kunihiro, Phys. Rept. **247**, 221 (1994), hep-ph/9401310.
- [24] D. Ebert, H. Reinhardt, and M. K. Volkov, Prog. Part. Nucl. Phys. **33**, 1 (1994).
- [25] M. K. Volkov, M. Nagy, and V. L. Yudichev, Nuovo Cim. **A112**, 225 (1999), hep-ph/9804347.
- [26] M. K. Volkov and A. E. Radzhabov, Phys. Usp. **49**, 551 (2006).
- [27] K. Kikkawa, Prog. Theor. Phys. **56**, 947 (1976).
- [28] M. K. Volkov and V. L. Yudichev, Phys. Part. Nucl. **31**, 282 (2000), hep-ph/9906371.
- [29] M. K. Volkov and A. A. Osipov, Sov. J. Nucl. Phys. **55**, 107 (1992).
- [30] D. V. Kreopalov and M. K. Volkov, Sov. J. Nucl. Phys. **37**, 770 (1983).